International Journal of Engineering Trends and Technology
ISSN: 2231–5381 / https://doi.org/10.14445/22315381/IJETT-V73I9P116

Volume 73 Issue 9, 186-193, September 2025

Original Article

Structural Stability Analysis of Composite Materials for High-Speed Shafts in Large-Capacity Wind Turbines

Yong-In Kim[1], Young-Kuk Kim[1], Yu-Jin Jeong[1], Min-Woo Kim[1], Hyoung-Woo Lee[2]

[1]*Department of Mechanical Engineering, Jungwon University, Republic of Korea, Chungbuk.*
[2]*Department of Unmanned Aeromechanical Engineering, Jungwon University, Republic of Korea, Chungbuk.*

[2]*Corresponding Author : @leehwoo@jwu.ac.kr*

Received: 22 April 2025 Revised: 08 September 2025 Accepted: 15 September 2025 Published: 30 September 2025

Abstract - *This study compares and analyzes key parameters of high-speed shaft couplings made from composite materials, focusing on the debonding area, the presence of pins, and the friction coefficient. High-speed shaft couplings are critical components of drivetrain systems, directly affecting the overall stability and reliability. Previous research has examined the design of high-speed couplings for a 6 MW wind turbine drivetrain. Building on this foundation, the present study evaluates the structural and mechanical performance of couplings under varying conditions. By systematically analyzing the effects of different debonding areas, the inclusion or exclusion of pins, and varying friction coefficients, this study aims to identify key factors influencing the coupling's reliability and efficiency. The findings are expected to contribute to the development of high-performance couplings for large-scale wind turbines, enhancing durability, operational stability, and long-term reliability.*

Keywords - *Wind turbine, Tsai-Wu strength index, High-speed shaft coupling, Debonding.*

1. Introduction

In wind power systems, high-speed shaft couplings must withstand high loads and repeated fatigue loads during power transmission, making them critical components. In particular, the reliability of couplings in large-scale wind turbines is directly related to the safety of the entire system, necessitating precise evaluation of their structural performance.

A typical wind turbine system consists of major components such as blades, gearbox, generator, and high-speed shaft. Among these, the high-speed shaft coupling plays a key role in transmitting power between the gearbox and the generator, and it is designed to endure high torque in a high-speed rotational environment.

Figure 1 shows the overall configuration of a wind turbine and the location of the high-speed shaft coupling. In large-capacity wind turbines, cases have been reported where debonding occurs in high-speed shaft couplings, leading to failure at the bonding interface [2].

Such defects may arise due to factors such as degradation of bonding durability, the presence or absence of pins, and variations in friction coefficient-each of which can significantly affect the long-term reliability of the coupling. The structural damage of the coupling can pose a serious threat to the long-term stable operation and performance of wind turbines.

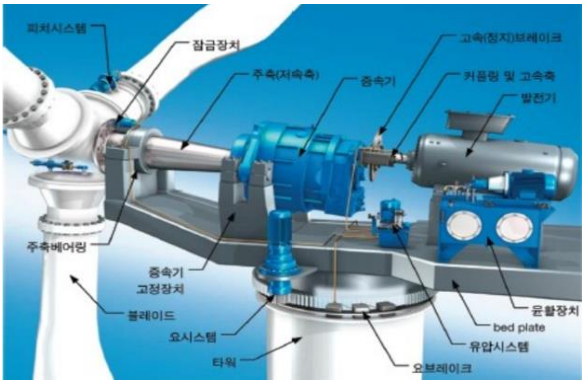

Fig. 1 Configuration of wind turbine system components [1]

Fig. 2 Failure of high-speed shaft coupling due to insufficient bonding strength

As shown in Figure 2, analyses of actual high-speed shaft coupling failures confirm that insufficient bonding strength can lead to interface damage. However, previous studies lack

a quantitative comparative analysis of how major design parameters-debonding area, presence of pins, and friction coefficient-affect the structural stability of composite couplings. Therefore, the objective of this study is to compare and analyze how the key parameters of composite high-speed shaft couplings influence their structural performance and reliability. To this end, Finite Element Analysis (FEA) and the Tsai-Wu failure theory are applied to evaluate stress distribution and potential failure under various conditions. This study is essential for the lightweight design of wind turbines and the structural stability of the coupling. The structure of this paper is as follows. Section 2 introduces the key parameters of composite high-speed shaft couplings and outlines the FEA methods used. Section 3 presents the results of structural stability assessments based on the presence of pins, debonding area, and changes in the friction coefficient, followed by a comparative analysis using the Tsai-Wu index. Finally, Section 4 summarizes the findings and suggests future research directions.

2. Analysis of Key Parameters in Composite High-Speed Shaft Couplings

High-speed shaft couplings in wind turbines serve as critical components that connect the generator and gearbox, transmitting high-speed rotational motion and torque while maintaining structural stability. In large-scale wind turbines, fatigue damage and deformation of couplings have emerged as major issues, prompting ongoing research into coupling designs using composite materials [3]. Traditionally, high-speed shaft couplings have been manufactured using metallic materials such as alloy steel. However, these metal couplings are heavy and suffer from reduced structural stability as fatigue damage accumulates. Consequently, recent studies have explored the use of lightweight composite materials-such as Glass Fiber-Reinforced Plastic (GFRP)-to design couplings that reduce weight while maintaining performance [4]. Ciprian Ionut Moraras et al. conducted tensile tests on Glass Fiber-Reinforced Polymers (GFRP) used in wind turbine blades. Through tensile testing according to the fiber orientation of GFRP, they proposed an optimal fiber arrangement that achieves maximum strength with minimal fiber usage [5]. Paul Bere et al. enhanced the mechanical properties of wind turbine blades by covering them with multiple layers of GFRP. By considering the stacking sequence of GFRP, they estimated the blade strength under operating loads and, based on numerical analysis results, characterized the structural strength of GFRP for blade manufacturing [6]. However, most studies on wind turbines utilizing composite materials have focused primarily on blades, while research on high-speed shaft couplings remains limited. Composite couplings offer excellent fatigue resistance and lightweight properties, and with proper design, can match or even exceed the strength and durability of conventional metal couplings.

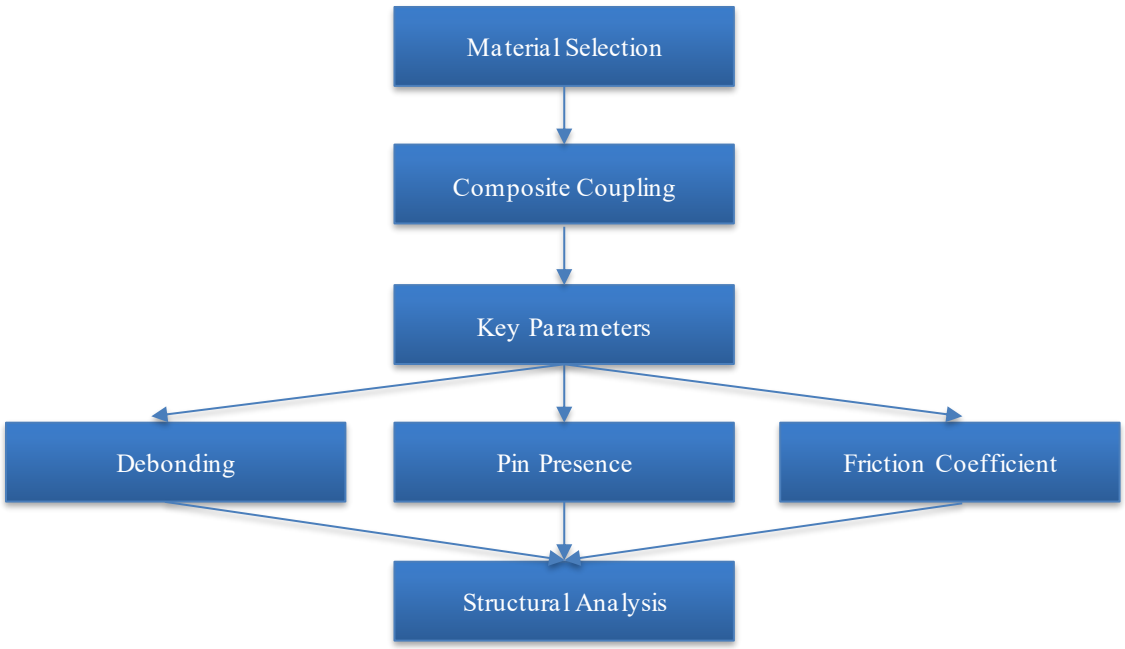

Fig. 3 High-speed shaft coupling diagram

Figure 3 presents a conceptual diagram summarizing the structure and main analytical components of the high-speed shaft coupling addressed in this study. The objective of this research is to compare and analyze key parameters that affect the structural stability of composite high-speed shaft couplings. Through this approach, we aim to assess whether composite couplings can meet the required performance standards in actual operating environments and to propose improved design strategies.

2.1. Definition of Key Parameters

The structural stability of high-speed shaft couplings is influenced by a variety of factors, among which the bonding area, supplemental reinforcement elements, and friction characteristics at contact surfaces have a direct impact on the coupling's reliability [7]. This study selects and analyzes three key parameters that influence the performance of high-speed shaft couplings:

The first parameter is the presence or absence of pins. One approach to addressing debonding issues involves reinforcing the structural joint by inserting pins. While the addition of pins may enhance the bonding strength between the flange and spacer, thereby improving stability, it may also result in stress concentrations around the pins, necessitating a detailed analysis. This study compares models with and without pin insertion to evaluate the impact of pin presence on the structural stability of the coupling [8]. The second parameter is the debonding area. In general, the spacer in a high-speed shaft coupling is bonded to the flange using adhesive. However, bonding degradation or repeated loading during operation may lead to a debonding phenomenon where the adhesive joint begins to separate. When debonding occurs, stress is likely to concentrate in the affected areas, potentially reducing structural stability and, in severe cases, leading to coupling failure. To assess this, the study sets debonding areas to 10 mm, 20 mm, and 30 mm and analyzes how reductions in bonding area affect the coupling's structural performance.

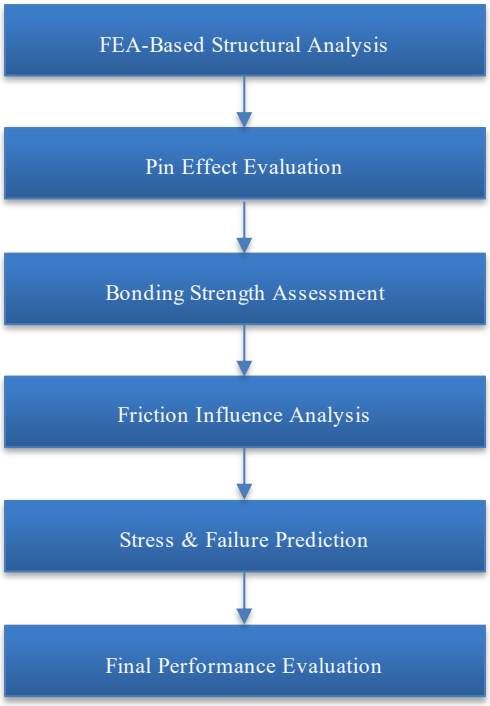

Fig. 4 Analysis workflow of high-speed shaft coupling using FEA

The third parameter is the coefficient of friction. The contact area and friction coefficient between internal components of the coupling are crucial elements that influence structural performance. In particular, the coefficient of friction between composite materials and metals varies depending on the joining method and surface condition, and it can change significantly if debonding occurs. This study establishes a baseline friction coefficient and then adjusts the range to evaluate structural performance under varying friction conditions. These processes are carried out according to the workflow shown in Figure 4 and are based on FEA.

2.2. Analysis Method and Conditions

In this study, FEA was employed to evaluate the structural performance of high-speed shaft couplings. ANSYS 2024 R1 was used as the analysis software, and an analysis model was constructed incorporating mesh settings, boundary conditions, and contact conditions to assess structural stability under various parameter changes.

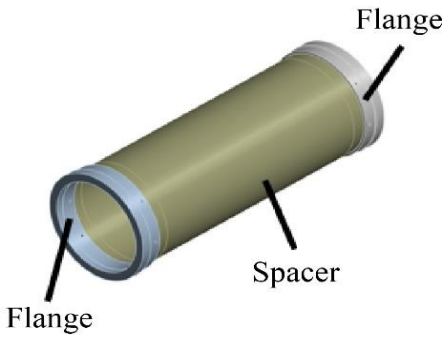

Fig. 5 Full model and simplified model of high-speed shaft coupling

The finite element model consists of the flange, spacer, and pin of the high-speed shaft coupling. To ensure accurate stress analysis, the Hex Dominant Mesh and the Multizone Method were applied. The analysis model shown in Figure 5 was simplified to enable more detailed post-processing of results through the use of ANSYS ACP (ANSYS Composite PrepPost), which allows efficient simulation of the structural properties of composite materials. As seen in Figure 6, considering the orthotropic properties of the material ensures uniform stiffness and can help alleviate debonding issues [9]. The basic mesh size was set to 10 mm, with finer meshes of 5 mm to 2 mm applied around the debonding region and pin interfaces to minimize mesh distortion and enhance the accuracy of the analysis. The simplified model consists of 504,019 nodes and 192,092 elements. For boundary conditions, one side of the flange was fixed as a Fixed Support, and a torque of 86,000 Nm was applied to the opposite side to simulate actual operating conditions, as illustrated in Figure 7. The material properties of the composite spacer and the SCM440 steel flange are listed in Tables 1 and 2, respectively. Frictional Contact was applied as the contact condition, and No Separation was applied to areas where bonding is maintained. This setup allows for a comparative analysis of stress variations and structural

stability changes depending on whether debonding occurs [4]. To evaluate the failure of the composite material, the Tsai-Wu failure criterion was applied [10]. If the Tsai-Wu index exceeds 1, it is considered indicative of material failure. The criterion can be expressed using Equation (1):

$$F_1\sigma_1 + F_2\sigma_2 + F_3\sigma_3 + F_4\sigma_4 + F_5\sigma_5 + F_6\sigma_6 + F_{11}{\sigma_1}^2 + F_{22}{\sigma_2}^2 + F_{33}{\sigma_3}^2 + F_{44}{\sigma_4}^2 + +F_{55}{\sigma_5}^2 + F_{66}{\sigma_6}^2 + 2F_{12}\sigma_1\sigma_2 + 2F_{13}\sigma_1\sigma_3 + 2F_{23}\sigma_2\sigma_3 \leq 1 \quad (1)$$

σ represents the stress components of the composite material, and F represents the strength coefficient. Using ANSYS APDL, the Tsai-Wu index was calculated, and the effects of debonding, presence or absence of pins, and variations in friction coefficient on the likelihood of failure were analyzed and compared. This study applies the aforementioned analytical methods to assess how each parameter affects the structural stability of high-speed shaft couplings and, based on the findings, aims to propose design strategies to ensure the reliability of composite couplings.

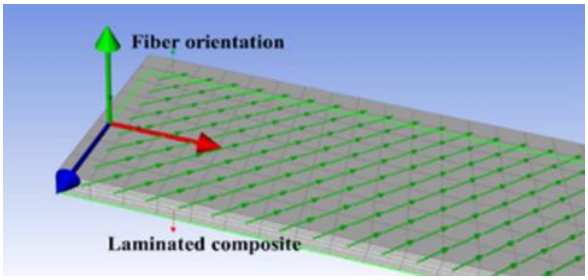

Fig. 6 Orthotropic cross-ply laminate example

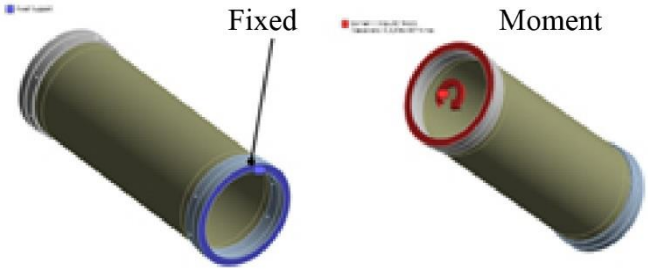

Fig. 7 Boundary conditions

Table 1. Equivalent material properties of composite

	Symbol	Unit	Value
Young′s Modulus	E1	GPa	43.4
	E2	GPa	12.1
	E3	GPa	12.1
Poisson′s Ratio	v12		0.294
	v23		0.294
	v13		0.294
Shear Modulus	G12	GPa	4.64
	G23	GPa	4.675
	G13	GPa	4.64

Table 2. Material properties of SCM440

	Symbol	Unit	Value
Young′s Modulus	E		210
Poisson′s Ratio	υ		0.3
Shear Modulus	Y	MPa	835
Tensile Strength	U_t	MPa	980

3. Results and Analysis

In this study, FEA was conducted to evaluate the structural stability of composite high-speed shaft couplings. The analysis model was developed using ANSYS 2024 R1, incorporating mesh settings, boundary conditions, and contact conditions to simulate real-world operating environments. The analysis results were compared across three key parameters, and structural stability was assessed by analyzing the Equivalent Stress, Maximum Principal Stress, and the Tsai-Wu Strength Index.

3.1. Analysis Results According to the Presence of Pins

Pin insertion is a design approach used to mitigate structural instability caused by debonding. This section analyzes the impact of the presence or absence of pins on the structural stability of the coupling [9]. The contact conditions for each case are illustrated in Figure 8, and the analysis results are shown in Figures 9 and 10. The stress values at the flange and spacer were 137.55 MPa and 103 MPa, respectively, for the model with pins, and 94.81 MPa and 88.33 MPa, respectively, for the model without pins. Although the model with pins showed slightly higher stress, the Tsai-Wu index, which is used to assess the likelihood of failure in composite materials, was 0.58 for the pinned model and 0.73 for the unpinned model. This indicates that the pinned model was safer in terms of composite material strength and behavior.

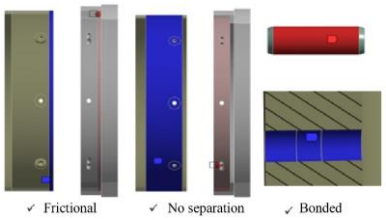

Pin Presence

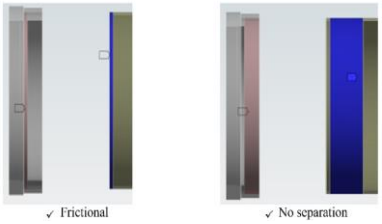

No Pin

Fig. 8 Contact conditions based on pin presence

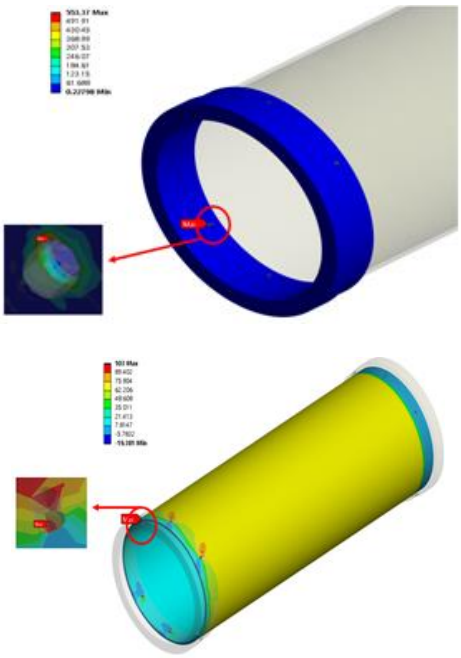

Fig. 9 FEA results with pin insertion

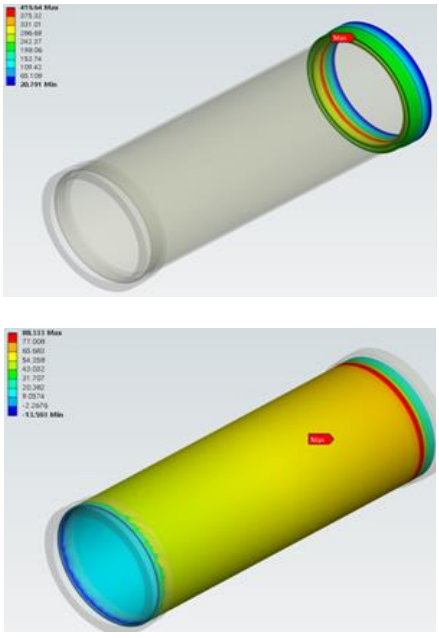

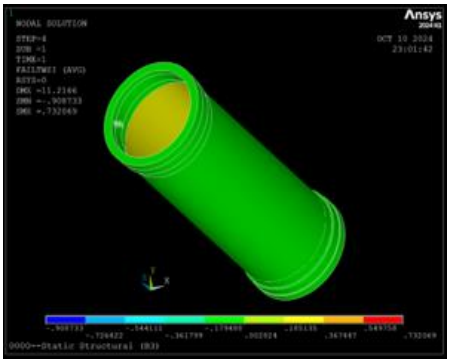

Fig. 10 FEA results without pin

This result demonstrates that the magnitude of stress and the strength, brittleness, and directional properties of composite materials must be comprehensively considered. The presence of fixed elements due to the inserted pin helps reduce the possibility of material failure.

3.2. Analysis Results According to Debonding Area Variation

Debonding refers to the weakening of structural bonding due to a decrease in adhesive strength. This section analyzes the effect of such debonding on the structural safety of the coupling [11]. The study evaluated three cases by setting the debonding area to 10 mm, 20 mm, and 30 mm, respectively. The setup is shown in Figure 11 [12]. Relative to the bonded area of the flange, the 20 mm and 30 mm debonding areas correspond to approximately 44% and 62% of the contact surface, respectively. The results are presented in Table 3 and Figure 12. For the 20 mm debonding area, the structure remained safe regardless of whether pins were present. However, in the 30 mm debonding case, the Tsai-Wu index exceeded 1.08 for the model without pins, indicating that failure had occurred.

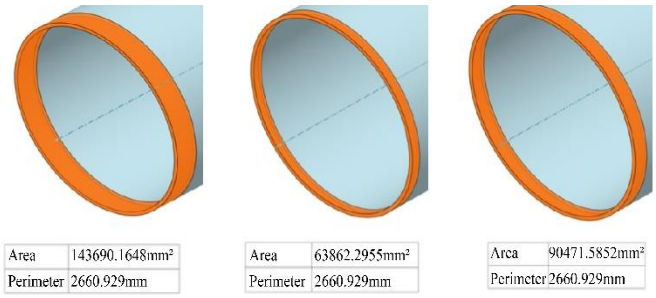

Area	143690.1648mm²
Perimeter	2660.929mm

Area	63862.2955mm²
Perimeter	2660.929mm

Area	90471.5852mm²
Perimeter	2660.929mm

Fig. 11 Comparison of different debonding areas

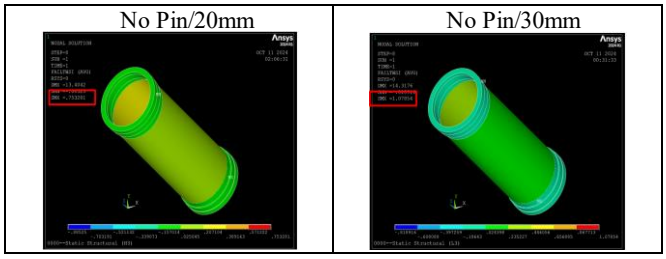

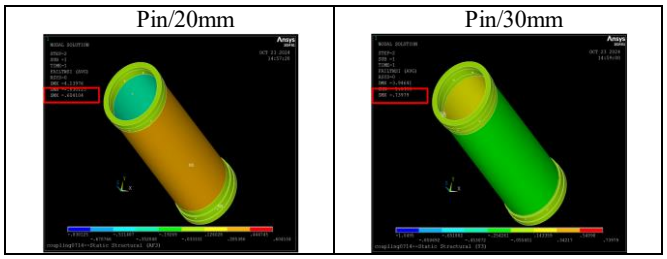

Fig. 12 20mm/30mm debonding tsai wu strength index

Table 3. Tsai-Wu strength index results for 20mm and 30mm debonding areas

	Ratio	Tsai-Wu
No Pin/20mm	44%	0.75
No Pin/30mm	62%	1.08
Pin/20mm	44%	0.60
Pin/30mm	62%	0.74

3.3. Analysis Results According to Changes in Friction Coefficient

The friction coefficient is a critical parameter that defines the contact characteristics within the coupling. This study analyzed how variations in the friction coefficient affect structural performance.

The base friction coefficient was set to 0.3, a value widely used in industry for stable torque transmission and durability, and it was considered validated for design purposes.

As shown in Figure 13, the range of friction coefficients used in the analysis was 0.11 to 0.415, reflecting realistic dry-condition interactions between GFRP and alloy steel (SCM 440), including frictional resistance and wear characteristics under the test conditions. The results for the Tsai-Wu index according to changes in friction coefficient are presented in Tables 4, 5, 6 and Figure 13.

In the case of a 10 mm debonding area with pins, the Tsai-Wu index ranged from 0.55 to 0.71 across the friction coefficient range of 0.11 to 0.415. As the friction coefficient increased, the index decreased. For the no-pin model, the index ranged from 0.57 to 0.78, showing a slightly higher tendency.

Under the 20 mm debonding condition, the pinned model showed values of 0.91 at a friction coefficient of 0.11 and 0.68 at 0.415, indicating an increase compared to the 10 mm case. For the no-pin model, safety was maintained at a friction coefficient of 0.2, but failure occurred at 0.11, with a Tsai-Wu index of 1.10.

Lastly, under the 30 mm debonding condition, the pinned model showed a relatively high value of 0.91 at 0.11, but remained below 1, indicating no failure. In contrast, the no-pin model exceeded 1 across the entire friction coefficient range (0.11–0.415), indicating structural failure. This FEA-focused analysis within a specific friction coefficient range confirmed that the presence of pins significantly contributes to structural stability.

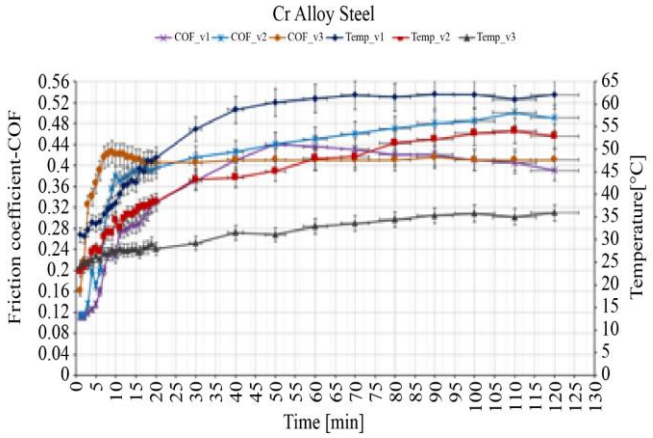

Fig. 13 Variation of friction coefficient between GFRP and alloy steel [13]

Table 4. 10mm friction coefficient analysis

Spacer	μ	Tsai-Wu strength index
Pin	0.11	0.71
	0.2	0.69
	0.3	0.57
	0.415	0.55
No Pin	0.11	0.78
	0.2	0.81
	0.3	0.73
	0.415	0.57

Table 5. 20mm friction coefficient analysis

Spacer	μ	Tsai-Wu strength index
Pin	0.11	0.83
	0.2	0.70
	0.3	0.60
	0.415	0.42
No Pin	0.11	1.10
	0.2	0.78
	0.3	0.75
	0.415	0.72

Table 6. 30mm friction coefficient analysis

Spacer	μ	Tsai-Wu strength index
Pin	0.11	0.91
	0.2	0.83
	0.3	0.73
	0.415	0.68
No Pin	0.11	1.37
	0.2	1.13
	0.3	1.08
	0.415	1.03

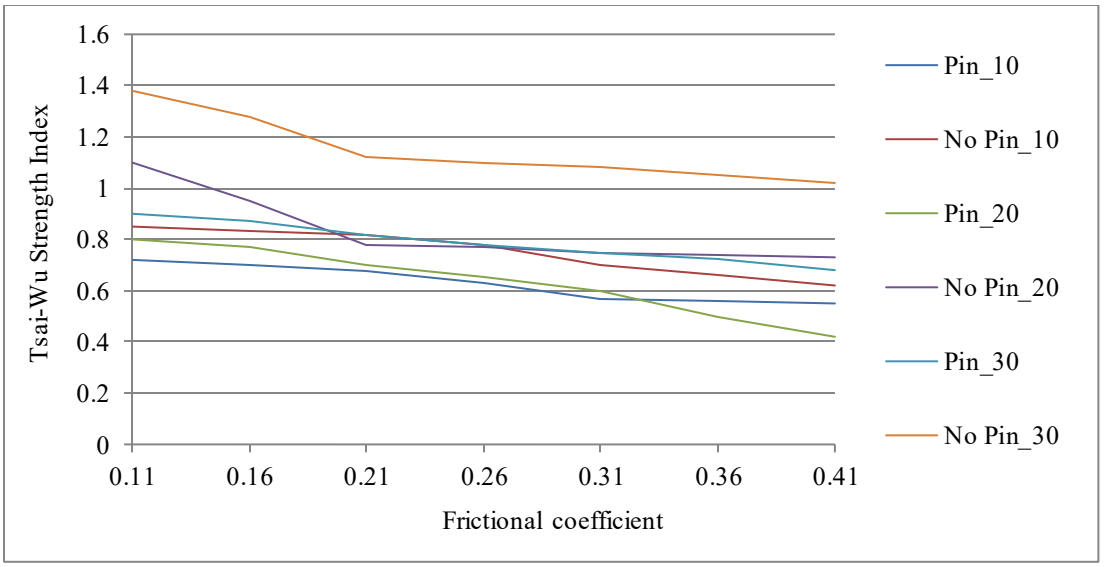

Fig. 14 Tsai-Wu strength index graph

4. Conclusion

This study comparatively analyzed the influence of three key parameters-presence of pins, debonding area, and friction coefficient-on the structural stability of composite high-speed shaft couplings. Using FEA, the stress distribution and Tsai-Wu index under various conditions were evaluated, and the effect of each parameter on the reliability and structural performance of the coupling was quantitatively assessed. The analysis showed that as the debonding area increased, the Equivalent Stress, Maximum Principal Stress, and Tsai-Wu index increased. In particular, when a 30 mm debonding occurred, the design stress limits were likely to be exceeded. This suggests that decreased bonding strength leads to stress concentration at the flange-spacer joint, increasing structural vulnerability. In the pin insertion analysis, it was confirmed that applying pins helped maintain structural stability even in the presence of debonding. On the other hand, in the no-pin model, stress increased due to reduced composite strength, and the Tsai-Wu index approached 1, indicating a higher likelihood of failure. Thus, pin insertion was found to be an effective design strategy for improving the reliability of composite couplings. Changes in the friction coefficient affected the coupling's bonding strength and load transfer characteristics. A lower friction coefficient weakened the bonding between the spacer and flange, resulting in greater stress concentration and a higher Tsai-Wu index. In particular, when the friction coefficient fell below 0.2, the risk of failure increased. However, the presence of pins eliminated this risk. Through this study, the structural characteristics of composite high-speed shaft couplings were quantitatively analyzed, and the effects of debonding prevention, pin insertion, and friction coefficient adjustment on reliability improvement were identified. This study contributes to the lightweight design and improved fatigue resistance of wind turbines, thereby demonstrating its potential to enhance structural stability. Future studies could further strengthen the practical applicability of composite couplings by incorporating experimental validation using real wind turbine operating data and analyzing the effects of dynamic loads and environmental changes, such as temperature variation.

References

[1] Korea Institute of Energy Research, New and Renewable Energy White Paper 2012, 2012. [Online]. Available: https://www.kier.re.kr/eng

[2] SonSeung Deok et al., "Development of High-Speed Coupling for 2MW Class Wind Turbine," *Journal of the Korean Society of Marine Engineering*, vol. 38, no. 3, pp. 262-268, 2014. [CrossRef] [Google Scholar] [Publisher Link]

[3] Le Ling, Yan Li, and Sicheng Fu, "A Reliability Analysis Strategy for the Main Shaft of a Wind Turbine using Importance Sampling and Kriging Model," *International Journal of Structural Integrity*, vol. 13, no. 2, pp. 297-308, 2022. [CrossRef] [Google Scholar] [Publisher Link]

[4] Joon-Ha Hwang et al., "Structural Analysis and Lightweight Optimization of a Buoyant Rotor-Type Permanent Magnet Generator for a Direct-Drive Wind Turbine," *Energies*, vol. 16, no. 15, pp. 1-16, 2023. [CrossRef] [Google Scholar] [Publisher Link]

[5] Ciprian Ionut Moraras et al., "Analysis of the Effect of Fiber Orientation on Mechanical and Elastic Characteristics at Axial Stresses of GFRP Used in Wind Turbine Blades," *Polymers*, vol. 15, no. 4, pp. 1-25, 2023. [CrossRef] [Google Scholar] [Publisher Link]

[6] Paul Bere et al., "Design and Manufacturing Method of GFRP Blades for Vertical Axis Wind Turbine," *IOP Conference Series: Materials Science and Engineering*, Prague, Czech Republic, vol. 1190, no. 1, pp. 1-10, 2021. [CrossRef] [Google Scholar] [Publisher Link]

[7] Zhanwei Li et al., "Dynamic Modeling and Analysis of Wind Turbine Drivetrain Considering the Effects of Non-Torque Loads," *Applied Mathematical Modelling*, vol. 83, pp. 146-168, 2020. [CrossRef] [Google Scholar] [Publisher Link]

[8] Syaiful, and Muchammad, "Analysis of the Effect of Turbine Operational Load on the Strength of Coupling Bolt Structure using the Finite Element Method," *International Research Journal of Innovations in Engineering and Technology*, vol. 8, no. 10, pp. 114-123, 2024. [CrossRef] [Publisher Link]

[9] Sarah David Müzel et al., "Application of the Finite Element Method in the Analysis of Composite Materials: A Review," *Polymers*, vol. 12, no. 4, pp. 1-59, 2020. [CrossRef] [Google Scholar] [Publisher Link]

[10] Xi Li et al., "Assessment of Failure Criteria and Damage Evolution Methods for Composite Laminates Under Low-Velocity Impact," *Composite Structures*, vol. 207, pp. 727-739, 2019. [CrossRef] [Google Scholar] [Publisher Link]

[11] Francesco Bianchi et al., "A Finite Element Model for Predicting the Static Strength of a Composite Hybrid Joint with Reinforcement Pins," *Materials*, vol. 16, no. 9, pp. 1-16, 2023. [CrossRef] [Google Scholar] [Publisher Link]

[12] Robert D. Adams, J. Comyn, and W.C. Wake, *Structural Adhesive Joints in Engineering*, Springer Netherlands, pp. 1-359, 1997. [Google Scholar] [Publisher Link]

[13] Corina Birleanu et al., "Tribo-Mechanical Investigation of Glass Fiber Reinforced Polymer Composites under Dry Conditions," *Polymers*, vol. 15, no. 6, pp. 1234-1245, 2023. [CrossRef] [Google Scholar] [Publisher Link]